Polymer Journal, Vol. 38, No. 12, pp. 1267–1277 (2006)

Wormlike Micelles of Binary Polyoxyethylene Alkyl Ether Mixtures $C_{10}E_6$ + $C_{14}E_6$ and $C_{14}E_8$ + $C_{14}E_6$

Yoshiyuki EINAGA,† Yumi KITO, and Mikiko WATANABE

Department of Chemistry, Nara Women's University, Nara 630-8506, Japan

(Received August 24, 2006; Accepted October 3, 2006; Published November 10, 2006)

ABSTRACT: The wormlike micelles formed with the binary mixtures of surfactant polyoxyethylene alkyl ethers (C_iE_j), $C_{10}E_6$ + $C_{14}E_6$ and $C_{14}E_8$ + $C_{14}E_6$, were characterized by static (SLS) and dynamic light scattering (DLS) experiments. The observed $Kc/\Delta R_0$ as a function of the surfactant concentration c have been successfully analyzed with the aid of the light scattering theory for micelle solutions, thereby yielding the molar mass $M_w(c)$ of the micelle as a function of c along with the cross-sectional diameter d of the micelle. The mean-square radius of gyration $\langle S^2 \rangle$ and the hydrodynamic radius R_H as functions of M_w have been well described by the theories for the wormlike spherocylinder model. The length of the micelles at fixed c and temperature T steeply increases with increasing weight fraction w_t of $C_{14}E_6$ in both of the surfactant mixtures, implying that the micelles greatly grow in length when the surfactant component with longer alkyl group or with shorter oxyethylene group increases in the mixture. The results are in line with the findings for the micelles of the single surfactant systems where the C_iE_j micelles grow in length to a greater extent for larger i and smaller j. Although the values of d do not significantly vary with composition of the surfactant mixture, the stiffness parameter λ^{-1} remarkably decreases with w_t in both of the mixtures, indicating that the stiffness of the micelle is controlled by the relative strength of the repulsive force due to the hydrophilic interactions between oxyethylen groups to the attractive one due to the hydrophobic interactions between alkyl groups among the surfactant molecules. [doi:10.1295/polymj.PJ2006100]

KEY WORDS Wormlike Micelle / Light Scattering / Phase Diagram / Radius of Gyration / Diffsion Coefficient / Hydrodynamic Radius / Polyoxyethylene Alkyl Ether / Surfactant /

Nonionic surfactant polyoxyethylene alkyl ethers $H(CH_2)_i(OCH_2CH_2)_jOH$ (abbreviated C_iE_j), form wormlike micelles in dilute aqueous solution of the L_1 phase at temperatures below the phase boundary of the LCST type. The polymer-like micelles grow in length with increasing surfactant concentration or with raising temperature. They have certain similarities to real polymers and have been, thus, characterized with the aid of the experimental techniques developed hitherto in the polymer solution field, such as static (SLS) and dynamic light scattering (DLS),[1–9] small-angle neutron scattering (SANS),[10–12] and so on.

In the previous papers,[13–19] we have also investigated micelle solutions of C_iE_j with various i and j by SLS and DLS measurements and viscometry. We have determined the values of $M_w(c)$ at a specified c along with the cross-sectional diameter d of the micelles from the analysis of the SLS data by using a molecular thermodynamic theory[20,21] formulated with the wormlike spherocylinder model. It has been then found that molar mass M_w dependence of the mean-square radius of gyration $\langle S^2 \rangle$, hydrodynamic radius R_H, and intrinsic viscosity $[\eta]$ is quantitatively represented by the chain statistical[22] and hydrodynamic[23–26] theories based on the wormlike chain and spherocylinder models, respectively, thereby yielding the values of the stiffness parameter λ^{-1}. These analyses have demonstrated that the C_iE_j micelles assume a shape of flexible cylinder.

Salient features found for the characteristics of C_iE_j micelles are summarized as:[17,19] (i) The micelles grow in length to a greater extent for larger i and smaller j. (ii) The d values do not significantly vary with the values of i and j. (iii) The stiffness parameter λ^{-1} decreases with increasing i at fixed j and increases with increasing j at fixed i. (iv) The spacing s between the adjacent hydrophilic tails of surfactant molecules on the micellar surface increases with increasing i and j. The results demonstrate that the characteristics of C_iE_j micelles varies considerably and delicately with the hydrophobic i and/or the hydrophilic chain length j of the surfactant molecules. In particular, the feature (i) may be considered to reflect that among surfactant molecules, attractive force due to the hydrophobic interactions which may contribute the micellar growth becomes stronger for larger i and repulsive force due to the hydrophilic interactions which may reduce the micellar size becomes stronger for larger j.

The present study extends the previous work[13–17,19] to the micelle solutions of the binary surfactant mixtures $C_{10}E_6$ + $C_{14}E_6$ and $C_{14}E_8$ + $C_{14}E_6$. The main aim is to investigate the effects of the hydrophobic

†To whom correspondence should be addressed (E-mail: einaga@cc.nara-wu.ac.jp).

and hydrophilic chain lengths, which is substantially changed with composition of the surfactant mixtures, on the micellar characteristics. In the former mixture, hydrophobic chain length i varies with composition at fixed hydrophilic chain length j, while in the latter, j varies with composition at fixed i.

EXPERIMENTAL

Materials

The surfactant $C_{10}E_6$, $C_{14}E_6$, and $C_{14}E_8$ samples were purchased from Nikko Chemicals Co. Ltd. and used without further purification. The solvent water used was high purity (ultrapure) water prepared with Simpli Lab water purification system of Millipore Co.

The micellar solutions were prepared by dissolving appropriate amount of the surfactant mixture of $C_{10}E_6 + C_{14}E_6$ or $C_{14}E_8 + C_{14}E_6$ with a given composition in water. Complete mixing and micelle formation were achieved by stirring using a magnetic stirrer at least for one day. The compositions for both of the surfactant mixtures are represented by the weight fraction w_t of $C_{14}E_6$ in the respective mixtures.

Phase Diagram

Cloud-point temperature of a given micelle solution was determined as the temperatures at which the intensity of the laser light transmitted through the solution abruptly decreased when temperature was gradually raised.

Static Light Scattering

SLS measurements were performed to obtain the weight-average molar mass M_w of the micelles of the surfactant mixtures $C_{10}E_6 + C_{14}E_6$ or $C_{14}E_8 + C_{14}E_6$. The scattering intensities were measured for dilute micelle solutions at various temperatures T. We have also determined the apparent mean-square radius of gyration $\langle S^2\rangle_{app}$ for the micelles at finite concentrations on the basis of the fundamental light scattering equation

$$\frac{Kc}{\Delta R_\theta} = \frac{1}{M_w(c)}\left(1 + \frac{1}{3}\langle S^2\rangle q^2\right) + 2A_2c + \cdots \quad (1)$$

by using the $M_w(c)$ values determined as described below. Here, c is the surfactant mass concentration, ΔR_θ is the excess Rayleigh ratio, and K is the optical constant defined as

$$K = \frac{4\pi^2 n^2 (\partial n/\partial c)_{T,p}^2}{N_A \lambda_0^4} \quad (2)$$

with N_A being the Avogadro's number, λ_0 the wavelength of the incident light in vacuum, n the refractive index of the solution, $(\partial n/\partial c)_{T,p}$ the refractive index increment, p the pressure, A_2 is the second virial coefficient and q is the magnitude of the scattering vector defined as

$$q = \frac{4\pi n}{\lambda_0}\sin(\theta/2) \quad (3)$$

The mean square radius of gyration $\langle S^2\rangle$ is denoted by $\langle S^2\rangle_{app}$, since it is possibly affected by intermicellar interactions at finite concentrations examined.

The apparatus used is an ALV DLS/SLS-5000/E light scattering photogoniometer and correlator system with vertically polarized incident light of 632.8 nm wavelength from a Uniphase Model 1145P He–Ne gas laser. The experimental procedure is the same as described before.[13–17,19] In the present study, we have treated the micelle solutions as the binary system which consists of micelles as a solute and water as a solvent.

The results for the refractive index increment $(\partial n/\partial c)_{T,p}$ measured at 632.8 nm with a Union Giken R601 differential refractometer are summarized as (in cm^3/g):

For micelle solutions of $C_{10}E_6 + C_{14}E_6$,

$$(\partial n/\partial c)_{T,p} = 0.132 - 1.72 \times 10^{-4}(T - 273.15) \quad (w_t = 0.250) \quad (4)$$

$$(\partial n/\partial c)_{T,p} = 0.129 - 6.33 \times 10^{-5}(T - 273.15) \quad (w_t = 0.502) \quad (5)$$

$$(\partial n/\partial c)_{T,p} = 0.135 - 1.72 \times 10^{-4}(T - 273.15) \quad (w_t = 0.752) \quad (6)$$

For micelle solutions of $C_{14}E_8 + C_{14}E_6$,

$$(\partial n/\partial c)_{T,p} = 0.1347 - 1.299 \times 10^{-4}(T - 273.15) \quad (w_t = 0.246) \quad (7)$$

$$(\partial n/\partial c)_{T,p} = 0.1404 - 2.169 \times 10^{-4}(T - 273.15) \quad (w_t = 0.498) \quad (8)$$

$$(\partial n/\partial c)_{T,p} = 0.1363 - 1.786 \times 10^{-4}(T - 273.15) \quad (w_t = 0.750) \quad (9)$$

Dynamic Light Scattering

DLS measurements were carried out to determine the translational diffusion coefficient D for the micelles by the use of the same apparatus and light source as used in the SLS studies described above. All the test solutions studied are the same as those used in the SLS studies. From the D values obtained by the cumulant method for the normalized autocorrelation function $g^{(2)}(t)$, the apparent hydrodynamic radius $R_{H,app}$ has been evaluated by the defining equation[13,27,28]

$$D = \frac{(1 - vc)^2 M_w k_B T}{6\pi\eta_0 R_{H.app}}\left(\frac{Kc}{\Delta R_0}\right) \quad (10)$$

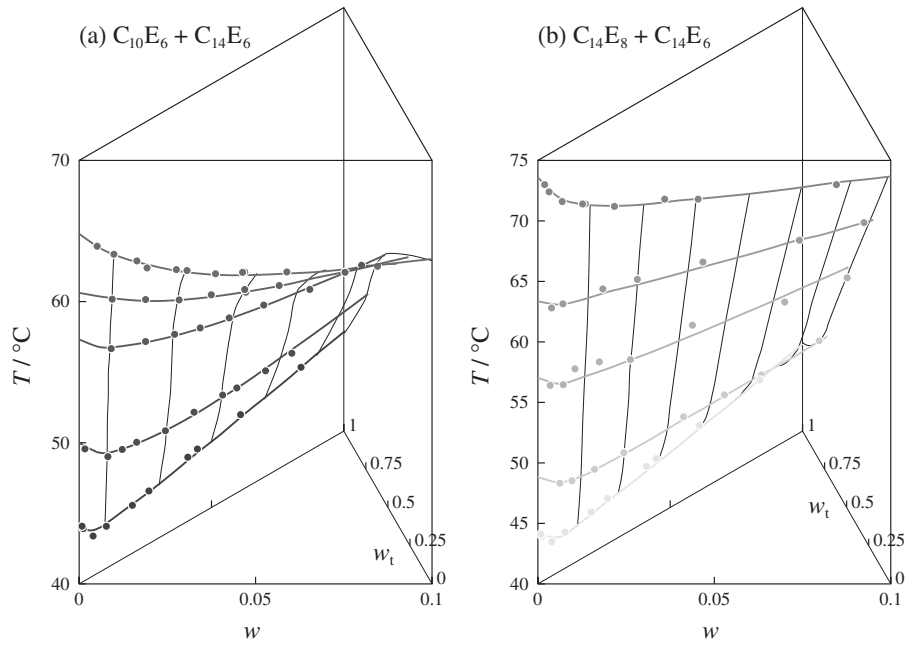

Figure 1. Three-dimensional representation of the binodal surface for micelle solutions of $C_{10}E_6 + C_{14}E_6$ (a) and $C_{14}E_8 + C_{14}E_6$ (b). Circles: observed cloud points. (a) The data points for $w_t = 0$ and 1 are the literature results of ref 15 and 13, respectively. (b) The data points for $w_t = 0$ and 1 are the literature results of ref 13 and 14, respectively.

where v is the partial specific volume of the solute (micelle), k_B is the Boltzmann constant, and η_0 is the solvent viscosity.

Density

The results for the solution density ρ determined with a picnometer of the Lipkin-Davison type are summarized as (in g/cm^3):

For micelle solutions of $C_{10}E_6 + C_{14}E_6$,

$$\rho^{-1} = 0.992 + 3.90 \times 10^{-4}(T - 273.15) - 0.016w \quad (w_t = 0.250) \tag{11}$$

$$\rho^{-1} = 0.991 + 4.23 \times 10^{-4}(T - 273.15) - 0.0227w \quad (w_t = 0.502) \tag{12}$$

$$\rho^{-1} = 0.995 + 3.39 \times 10^{-4}(T - 273.15) - 0.0227w \quad (w_t = 0.752) \tag{13}$$

For micelle solutions of $C_{14}E_8 + C_{14}E_6$,

$$\rho^{-1} = 0.9921 + 3.832 \times 10^{-4}(T - 273.15) - 0.0328w \quad (w_t = 0.246) \tag{14}$$

$$\rho^{-1} = 0.9921 + 3.831 \times 10^{-4}(T - 273.15) \quad (w_t = 0.498) \tag{15}$$

$$\rho^{-1} = 0.9952 + 3.153 \times 10^{-4}(T - 273.15) - 0.0226w \quad (w_t = 0.750) \tag{16}$$

where w is the weight fraction of the surfactant mixtures in the micelle solution. The values of v of the micelles have been calculated from the above results by the equation

$$\rho^{-1} = \rho_0^{-1} + (v - \rho_0^{-1})w \tag{17}$$

with ρ_0 being the ρ value of the pure water.

RESULTS AND DISCUSSION

Phase Behavior

Figure 1 illustrates the 3D phase diagrams for the aqueous solutions of $C_{10}E_6 + C_{14}E_6$ (a) and $C_{14}E_8 + C_{14}E_6$ (b), along with the literature results at $w_t = 0$ and $w_t = 1$.[13–15] It is seen that all the micelle solutions studied represent the phase separation behavior of the LCST (lower critical solution temperature) type and that the phase boundaries significantly shift to lower temperatures as w_t increases, or in other word, the component of the larger i increases at fixed j or the component of the smaller j increases at fixed i in the surfactant mixtures.

The phase behavior resembles the observations for real polymer solutions, in which the phase boundary of the LCST type is shifted to lower temperatures with increasing polymer molecular weight. Thus, the present results suggest that the micellar size becomes larger as the component of the longer hydrophobic chain length or of the shorter hydrophilic chain length increases in the surfactant mixtures. All the light scattering measurements were made in the single phase region at temperatures below the phase boundary shown in Figures 1a and 1b.

Analysis of the SLS Data

In order to determine the M_w values of the micelles at a specific concentration c, we have analyzed the present SLS data by employing a light-scattering theory for micellar solutions formulated by Sato[20,21] with wormlike spherocylinder model for polymer-like micelles. The model consists of a wormlike cylinder of contour length $L - d$ with cross-sectional diameter d and two hemispheres of diameter d which cap both ends of the cylinder, and stiffness of the wormlike cylinder is represented by the stiffness parameter λ^{-1}. The result for $Kc/\Delta R_0$ reads

$$\frac{Kc}{\Delta R_0} = \frac{1}{M_w(c)} + 2A(c)c \tag{18}$$

where $M_w(c)$ is the weight-average molar mass of the micelles and $A(c)$ is the apparent second virial coefficient in a sense that it is comprised of the second, third, and the higher virial coefficient terms. $M_w(c)$ and $A(c)$ are functions of c, containing three parameters d, free-energy parameter g_2 which controls micellar growth, and strength $\hat{\epsilon}$ of the attractive interaction between spherocylinders. We refer the expressions for the functions $M_w(c)$ and $A(c)$ to the original papers (ref 20 and 21) and our previous papers,[13,15] since they are fairly involved.

As mentioned above, we have treated present micelle solutions as two component systems consisting of micelles and solvent, although they include two types of surfactant molecules and water. It has been assumed in the analyses that the surfactant composition in the micelles is the same as a given value of w_t.

Figures 2 and 3 demonstrate the results of curve-fitting of the theoretical calculations to the experimental values of $Kc/\Delta R_0$ for the micelle solutions of $C_{10}E_6 + C_{14}E_6$ and $C_{14}E_8 + C_{14}E_6$, respectively, at indicated temperatures and at three w_t's. The solid curves in the figures represent the best-fit theoretical values. We find that they are in good coincidence with the respective data points at given temperatures. The good agreement implies that the micelles of the two surfactant mixtures in dilute aqueous solutions are represented by the wormlike spherocylinder model. The dashed lines represent the values of $1/M_w(c)$ at respective temperatures. For all the micelles at any fixed w_t and T, they are straight lines with a slope of -0.5, showing that M_w increases with c following a relation $M_w \propto c^{1/2}$ in the range of c examined, as in the case of the previous findings[13–17,19] for the micelles formed with single surfactant of various type. These results are in good correspondence with simple theoretical predictions derived from the thermodynamic treatments of multiple equilibria among micelles of various aggregation numbers.[20,29–31] The solid and dashed curves coincide with each other at small c and the difference between them steadily increases with increasing c. The results indicate that contributions of the virial coefficient terms, that is, the second term of the right hand side of eq 18, to $Kc/\Delta R_0$ are negligible at small c but progressively increase with increasing c as expected.

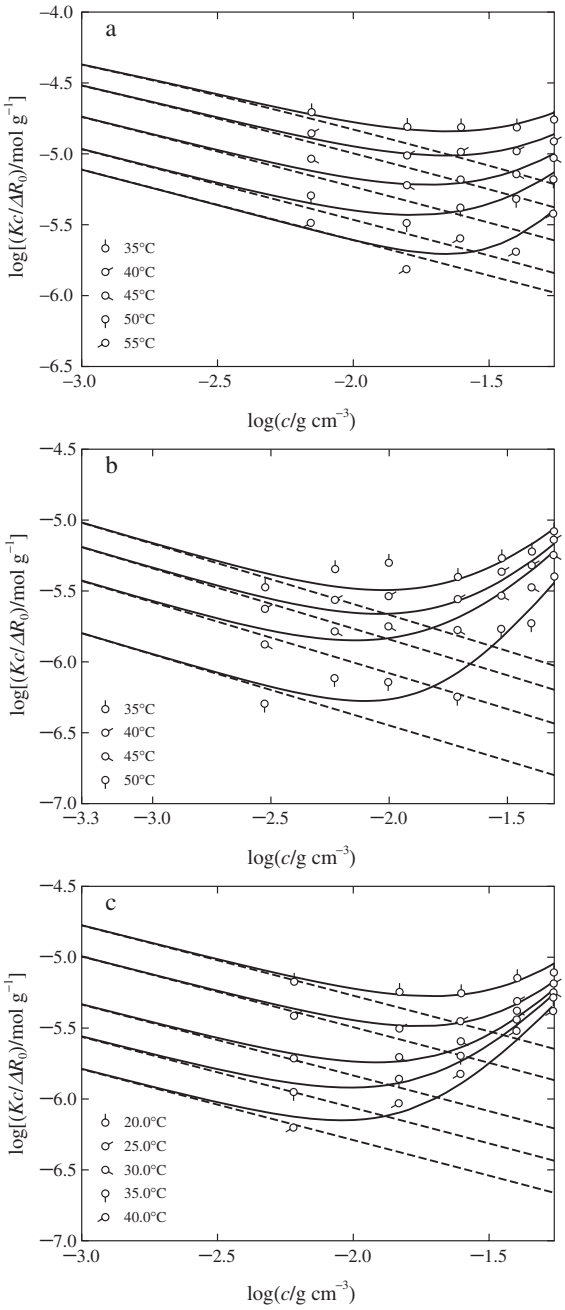

Figure 2. The results of the curve fitting for the plots of $Kc/\Delta R_0$ against c for micelle solutions of $C_{10}E_6 + C_{14}E_6$ with $w_t = 0.250$ (a), 0.502 (b), and 0.752 (c) at various temperatures indicated: The solid and dashed curves represent the calculated values of $Kc/\Delta R_0$ and $1/M_w(c)$, respectively.

The d values obtained for the micelles of the two surfactant mixtures are listed in Table I. They were independent of T and slightly varied with w_t. The lat-

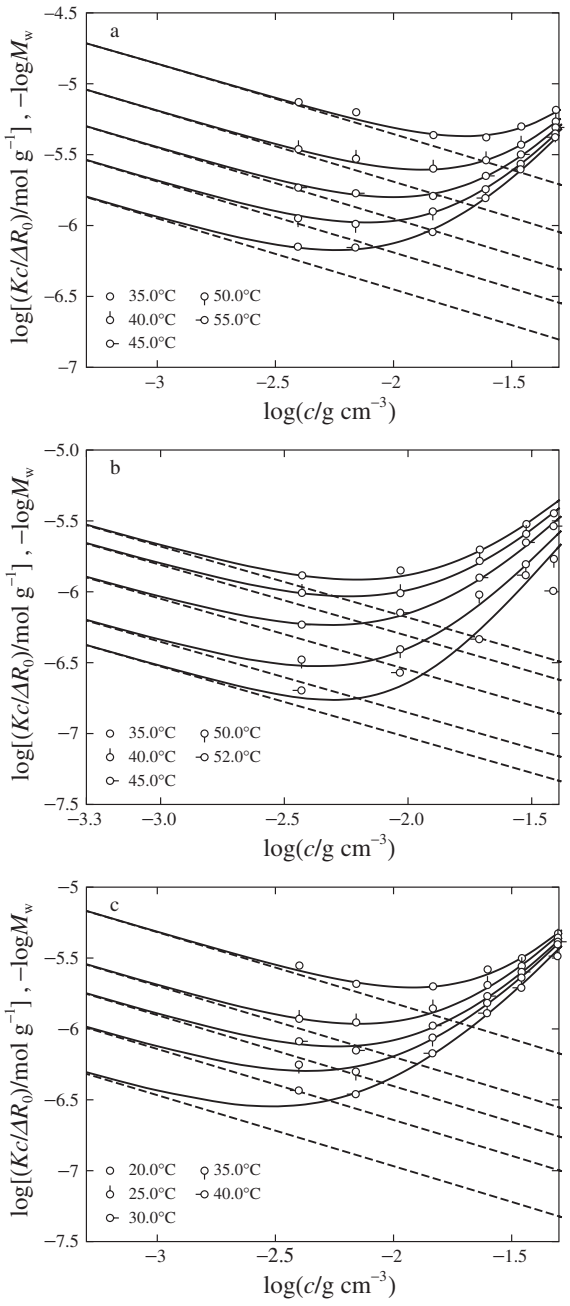

Figure 3. The results of the curve fitting for the plots of $Kc/\Delta R_0$ against c for micelle solutions of $C_{14}E_8 + C_{14}E_6$ with $w_t = 0.246$ (a), 0.498 (b), and 0.750 (c) at various temperatures indicated: The solid and dashed curves represent the calculated values of $Kc/\Delta R_0$ and $1/M_w(c)$, respectively.

ter results suggest that the alkyl and oxyethylene groups of the C_iE_j molecule do not assume a straight form with all trans zig-zag conformation but a randomly coiled form in the micelles.

For the micelle solutions of both surfactant mixtures, g_2 is an increasing function of T and w_t, though they are not graphically shown here. It implies that the g_2 value becomes larger as the surfactant component with larger i or smaller j increases in the surfactant mixtures. On the other hand, $\hat{\epsilon}$ does not show clear systematic dependence on the surfactant species, taking roughly a constant value $\hat{\epsilon}/k_BT \simeq 0.3 \pm 0.1$.

Table I. The Micellar Characteristics

$C_{10}E_6 + C_{14}E_6$ micelles			
w_t	d/nm	λ^{-1}/nm	s/nm
0[a]	2.6	75	1.20
0.250	2.6	27	1.20
0.502	2.5	19	1.23
0.752	2.5	11	1.26
1[b]	2.4	7	1.30
$C_{14}E_8 + C_{14}E_6$ micelles			
w_t	d/nm	λ^{-1}/nm	s/nm
0[c]	2.3	18	1.46
0.246	2.6	17	1.32
0.498	2.6	12	1.31
0.750	2.8	16	1.23
1[b]	2.4	7	1.30

[a]cited from ref 15. [b]cited from ref 13. [c]cited from ref 14.

Hydrodynamic Radius of the Micelles

The values of $R_{H,app}$ have been determined by eq 10 at various w_t, T, and c for the micelles of $C_{10}E_6 + C_{14}E_6$ and $C_{14}E_8 + C_{14}E_6$. We have found that at any given w_t and T, $R_{H,app}$ increases with increasing c, although the results are not shown here. The $R_{H,app}$ values, however, do not necessarily correspond to those for "isolated" micelles, since they reflect both micellar growth in size and enhancement of the effects of the intermicellar hydrodynamic interactions with increasing c.

Figures 4 and 5 depict double-logarithmic plots of $R_{H,app}$ against M_w for the micelles of $C_{10}E_6 + C_{14}E_6$ and $C_{14}E_8 + C_{14}E_6$, respectively. In our previous papers,[13–15] it has been shown that in similar plots, the data points at different T asymptotically form a single composite curve at low c, or small M_w, implying that the effects of the intermicellar hydrodynamic interactions on $R_{H,app}$ become negligible in the asymptotic region of low c. The present results are similar to the previous findings. We, therefore, analyze the data points at the smallest M_w at each fixed T in Figures 4 and 5 by regarding them to provide the relationship between R_H and M_w for "isolated" micelles.

In the present analyses, we have employed the equations formulated by Norisuye, *et al.*[23] for the wormlike spherocylinder model near the rod limit and by Yamakawa, *et al.*[24,25] for the wormlike cylinder model, as a function of L with including the parameters d and λ^{-1}. We have combined these theoretical results in order to calculate R_H over the entire range of L including the sphere, *i.e.*, the case $L = d$. The equation for R_H reads

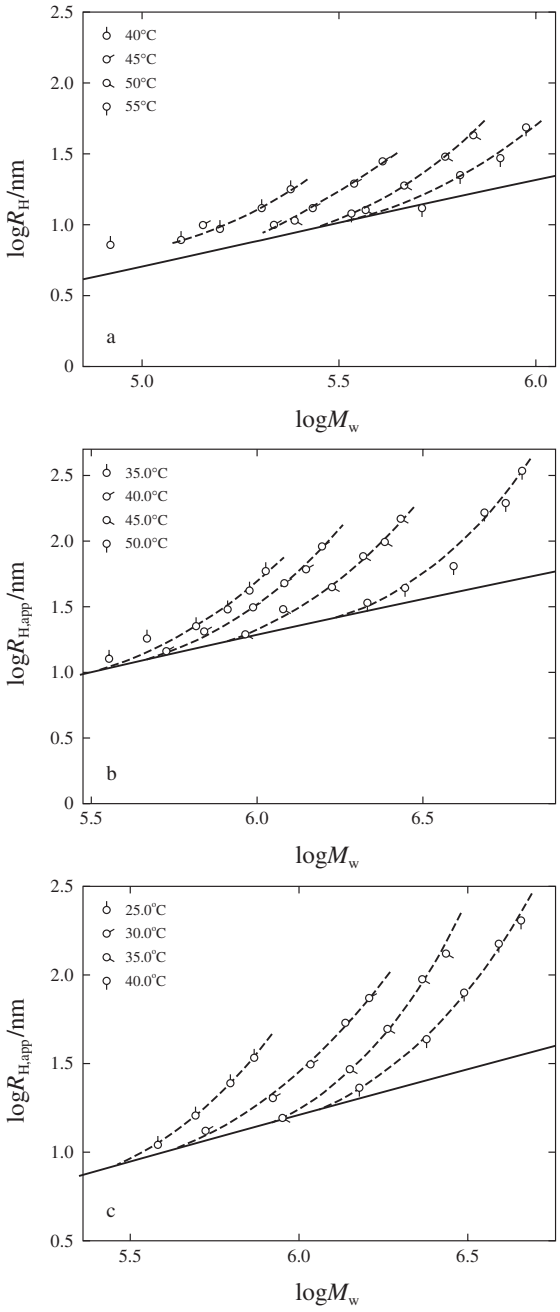

Figure 4. Double-logarithmic plots of $R_{H,app}$ against M_w for the micelles of $C_{10}E_6 + C_{14}E_6$ with $w_t = 0.250$ (a), 0.502 (b), and 0.752 (c) at various temperatures indicated: The dashed curves are drawn to guide the eye. The solid curve represents the theoretical values calculated by eqs 19 and 20.

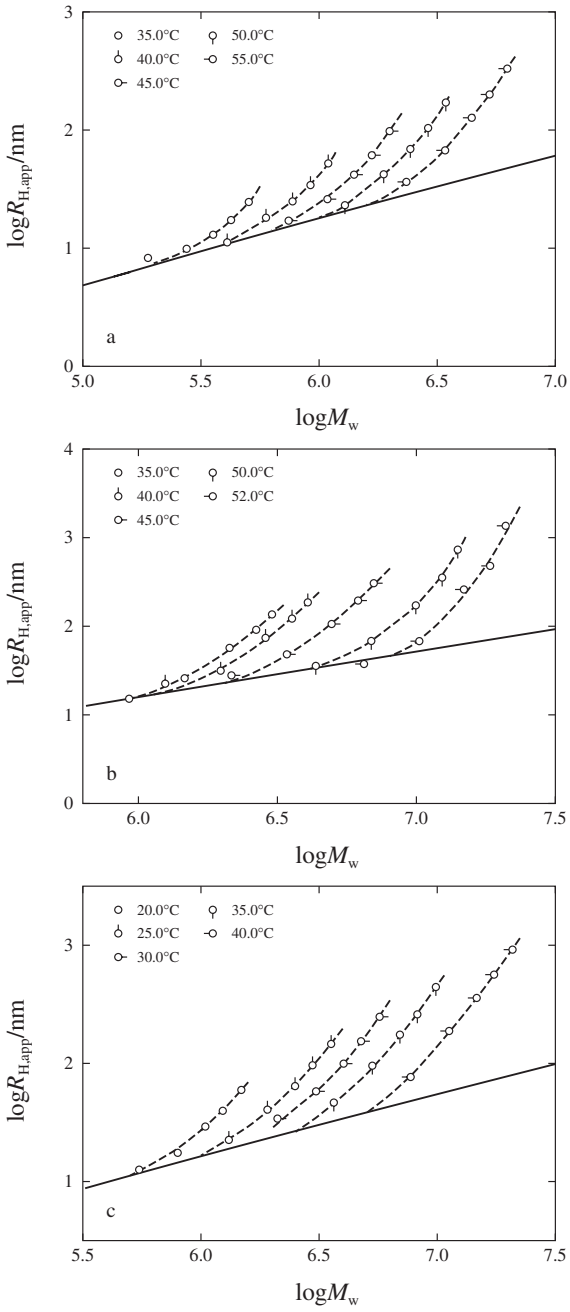

Figure 5. Double-logarithmic plots of $R_{H,app}$ against M_w for the micelles of $C_{14}E_8 + C_{14}E_6$ with $w_t = 0.246$ (a), 0.498 (b), and 0.750 (c) at various temperatures indicated: The dashed curves are drawn to guide the eye. The solid curve represents the theoretical values calculated by eqs 19 and 20.

$$R_H = \frac{L}{2f(\lambda L, \lambda d)} \tag{19}$$

The expression for the function f is so lengthy that we refer it to the original papers.[23–25] The weight-average micellar length L_w is related to M_w by

$$L_w = \frac{4\nu M_w}{\pi N_A d^2} + \frac{d}{3} \tag{20}$$

Here, the relation between L_w and M_w is derived from the micellar volume and L_w is used in place of L in eq 19. By eqs 19 and 20, the values of R_H have been theoretically calculated as a function of M_w for various values of λ^{-1} with the use of the d values determined above from the SLS results.

The solid lines in Figures 4 and 5 represent best-fit curves to the data points for the micelles of the smallest M_w for the two surfactant mixtures with given w_t and T. It is found that the theoretical curves well describe the observed behavior of R_H as a function of M_w, implying that the micelles may be represented

with the wormlike spherocylinder model, although the data point for $C_{10}E_6 + C_{14}E_6$ with $w_t = 0.250$ at $T = 40.0\,^{\circ}C$ deviates upward for unknown reasons at present. The data points at fixed T steeply increase with M_w deviating upward from the solid curve due to the enhancement of the intermicellar hydrodynamic interactions with increasing c.

The λ^{-1} values obtained from the curve fittings are summarized in Table I along with the values of d. In the Table, it is found that the λ^{-1} values for the micelles of both surfactant mixtures are greatly decreased with increasing w_t. In other words, the stiffness of the micelles of $C_{10}E_6 + C_{14}E_6$ decreases with increasing C_iE_j component with larger i and that of the micelles of $C_{14}E_8 + C_{14}E_6$ decreases with increasing C_iE_j component with smaller j. These results are in line with the findings[17,19] for the micelles formed with the single surfactant C_iE_j, in which λ^{-1} decreases with increasing i at fixed j and increases with increasing j at fixed i. They are also similar to our recent results for the micelles of the binary surfactant systems $C_{10}E_5 + C_{14}E_5$ and $C_{14}E_5 + C_{14}E_7$.[32]

It may be concluded that the relative strength of the repulsive force due to the hydrophilic interaction among C_iE_j molecules in the micelle to the attractive force due to the hydrophobic interactions controls the stiffness parameter; the repulsive force between the adjacent oxyethylene chains contribute to make the micelles stiffer and the attractive force between the adjacent alkyl chains reduce stiffness. The dependence of λ^{-1} on the hydrophilic chain length shows a striking resemblance to the results for regular-comb polymers or polymacromonomers in which the stiffness of the polymers is significantly increased with increasing side-chain length.[33] Nakamura and Norisuye[33] have theoretically showed that the remarkable enhancement of the stiffness is caused by excluded-volume interactions among side chains. Their treatment may also be applied to the present case for the variation of λ^{-1} with oxyethylene chain length. On the other hand, the variation of λ^{-1} with alkyl chain length still remains as a challenging issue.

Radius of Gyration

In Figures 6 and 7, $\langle S^2\rangle_{app}^{1/2}$ is double-logarithmically plotted against M_w for the micelles of $C_{10}E_6 + C_{14}E_6$ and $C_{14}E_8 + C_{14}E_6$, respectively. We note that $\langle S^2\rangle_{app}^{1/2}$ for the micelles of the former mixtures with $w_t = 0.250$ is not large enough to be determined by light scattering. For the micelles of each system, the data points at various T and c are found to form a single composite curve, suggesting that the values of $\langle S^2\rangle_{app}^{1/2}$ determined at finite c correspond to those of $\langle S^2\rangle^{1/2}$ for the individual micelles free from inter- and intramicellar interactions or excluded volume effects.

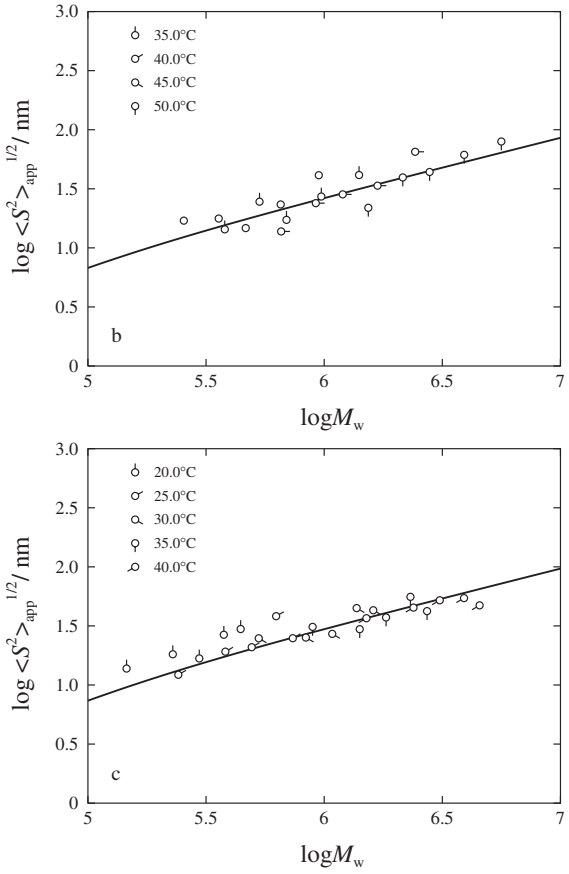

Figure 6. Double-logarithmic plots of $\langle S^2\rangle_{app}^{1/2}$ against M_w for the micelles of $C_{10}E_6 + C_{14}E_6$ with $w_t = 0.502$ (b) and 752 (c) at indicated temperatures. The solid curve represents the theoretical values calculated by eqs 20 and 21.

Thus, we have analyzed them by using the equation for the wormlike chain[22]

$$\lambda^2\langle S^2\rangle = \frac{\lambda L}{6} - \frac{1}{4} + \frac{1}{4\lambda L} - \frac{1}{8\lambda^2 L^2}(1 - e^{-2\lambda L}) \quad (21)$$

The solid curves in Figures 6 and 7 show the best-fit theoretical values of $\langle S^2\rangle^{1/2}$ for each micelle. Here, L_w by eq 20 is used in place of L in eq 21 and we have used the values of d determined above from the analyses of the SLS data. It is found that the calculated results well explains the observed behavior of $\langle S^2\rangle_{app}^{1/2}$. This agreement again shows that the micelles of the present surfactant mixtures assume a shape of wormlike spherocylinder. The values of λ^{-1} evaluated by these curve fittings are 20 and 16 nm for the micelles of $C_{10}E_6 + C_{14}E_6$ with $w_t = 0.502$ and 0.752, respectively, and 17, 17, and 20 nm for the micelles of $C_{14}E_8 + C_{14}E_6$ with $w_t = 0.246$, 0.498, and 0.750, respectively. They are somewhat larger than those obtained above from the analyses of the hydrodynamic radius R_H. This difference may be attributed to the fact that there is a distribution in micellar size and different averages are reflected in $\langle S^2\rangle_{app}^{1/2}$ and R_H. Sato[20] and Zoeller, *et al.*[31] have theoretically shown that

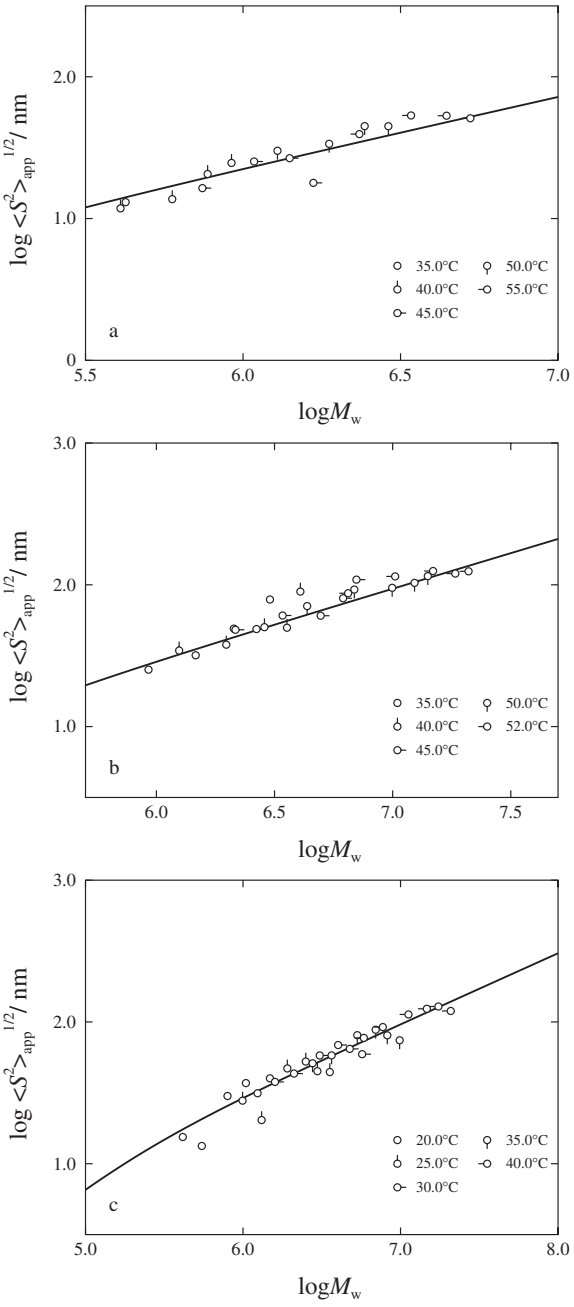

Figure 7. Double-logarithmic plots of $\langle S^2 \rangle_{app}^{1/2}$ against M_w for the micelles of $C_{14}E_8 + C_{14}E_6$ with $w_t = 0.246$ (a), 0.498 (b), and 0.750 (c) (c) at various temperatures indicated. The solid curve represents the theoretical values calculated by eqs 20 and 21.

micelles with sufficiently large aggregation number N have the most probable distribution. Quite recently, Sato[34] has showed that the distribution largely affects the evaluation of λ^{-1} from $\langle S^2 \rangle^{1/2}$ and that both of the λ^{-1} values from $\langle S^2 \rangle^{1/2}$ and R_H become comparable to each other when the effect of the micellar size distribution is taken into account.

The Micellar Length

The weight-average micellar length L_w have been calculated by eq 20 from the values of $M_w(c)$ and d obtained above from the analyses of the SLS data. The results at fixed T are shown in Figure 8 as functions of c and w_t, and in Figure 9, those at fixed c are shown as functions of T and w_t. Here, the previous results for the $C_{10}E_6$, $C_{14}E_6$, and $C_{14}E_8$ micelles are reproduced as the data points at $w_t = 0$ or 1.0 from the literature.[13–15] For all the micelles at a given w_t, L_w becomes larger as c is increased or T is raised.

As found in Figures 8a and 9a, the micellar length L_w at fixed c or at fixed T steeply increases with increasing w_t, *i.e.*, as the surfactant component with longer alkyl chain length i increases in the surfactant mixtures. This finding may be interpreted as follows. In the surfactant mixtures $C_{10}E_6 + C_{14}E_6$, the number of the oxyethylene units in the hydrophilic group is fixed to 6 irrespective of w_t and then the strength in the repulsive force between the adjacent oxyethylene chains may remain constant for different surfactant mixtures. On the other hand, attractive force among alkyl chains of the surfactant molecules due to the hydrophobic interactions is considered to become stronger as the amount of the component with larger i is increased. The effects may facilitate the growth of micelles to the greater length for this surfactant mixture with increasing the component with longer alkyl chain.

In Figures 8b and 9b, it is seen that the length L_w of the micelles of the mixtures $C_{14}E_8 + C_{14}E_6$ becomes longer with increasing w_t or increasing the component with shorter oxyethylene chain length j at fixed i. Since water is a good solvent for polyoxyethylene, the oxyethylene group of the surfactant C_iE_j molecule is playing a role to stabilizes the micelle in water. The affinity among the oxyethylene groups and water molecules causes repulsive force between the adjacent oxyethylene chains on the surface of the micelle, for the one end of the chain is fixed to the micelle core. The repulsive force is considered to be stronger for longer the oxyethylene group and it works to make more surface area of the micelle, resulting in the shorter micelles. This may explain the results that the micelles of $C_{14}E_8 + C_{14}E_6$ become longer as the component with smaller j is increased in the surfactant mixtures.

Characteristics of the Micelles

The values of the spacing s between the hydrophilic tails of adjacent surfactant molecules on the micellar surface are evaluated from the values of d, L_w, and the aggregation number N_w calculated from M_w. They are summarized in Table I along with the the results for d and λ^{-1}. We find that the s value does not significantly vary with w_t for the micelles of $C_{10}E_6 + C_{14}E_6$ and $C_{14}E_8 + C_{14}E_6$: It slightly increases with w_t in the former and slightly decreases with increasing

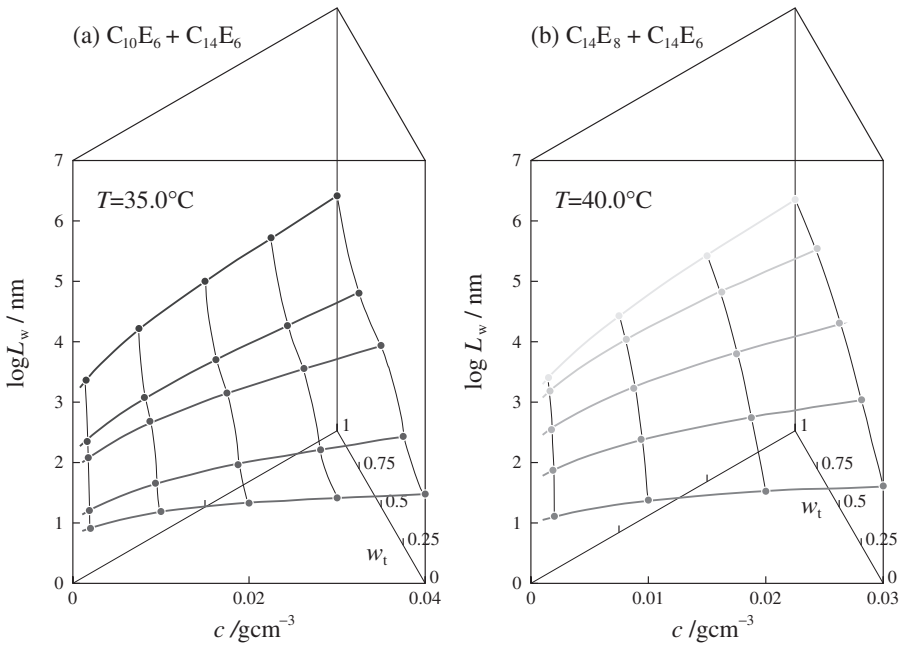

Figure 8. Concentration and w_t dependence of L_w for the micelles of $C_{10}E_6 + C_{14}E_6$ (a) at 35.0 °C and $C_{14}E_8 + C_{14}E_6$ (b) at 40.0 °C: (a) The data points for $w_t = 0$ and $w_t = 1$ are the results of ref 15 and 13, respectively. (b) The data points for $w_t = 0$ and $w_t = 1$ are the results of ref 13 and 14, respectively.

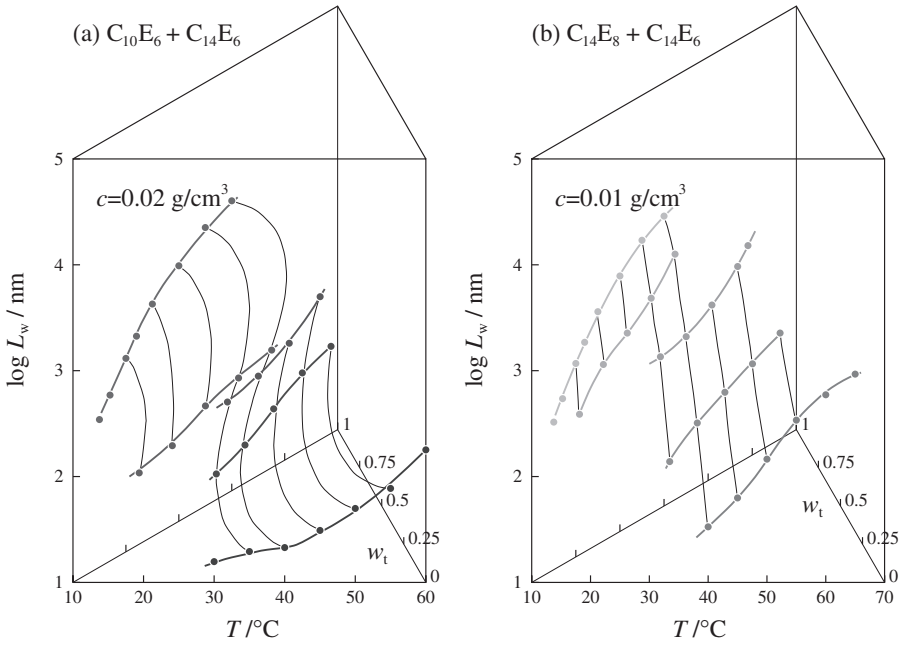

Figure 9. Temperature and w_t dependence of L_w for the micelles of $C_{10}E_6 + C_{14}E_6$ (a) at $c = 0.02$ g/cm^3 and $C_{14}E_8 + C_{14}E_6$ (b) at $c = 0.01$ g/cm^3: (a) The data points for $w_t = 0$ and are the results of ref 15 and 13, respectively. (b) The data points for $w_t = 0$ and 1 are the results of ref 13 and 14, respectively.

w_t in the latter.

In the surfactant mixture $C_{10}E_6 + C_{14}E_6$ with $w_t = 0.502$, the weight-average alkyl chain length is close to 12 and the oxyethylene chain length is fixed to 6. On the other hand, the weight-average oxyethylene chain length of the surfactant mixture $C_{14}E_8 + C_{14}E_6$ with $w_t = 0.498$ is approximately 7 and the alkyl chain length is fixed at 14. It may be, thus, significant to make comparison of the characteristics of the former micelle with that of the micelle of the single surfactant $C_{12}E_6$,[13] and that of the latter micelle with that of the micelle of the single surfactant $C_{14}E_7$.[17] The comparison is made in Table II for the values of d, λ^{-1}, and s. We find that the micelles of

Table II. Comparison of the micellar characteristics

	$C_{10}E_6 + C_{14}E_6$ ($w_t = 0.502$) micelle	$C_{12}E_6$ micelle[a]
d/nm	2.5	2.3
λ^{-1}/nm	19	14
s/nm	1.23	1.30

	$C_{14}E_8 + C_{14}E_6$ ($w_t = 0.498$) micelle	$C_{14}E_7$ micelle[b]
d/nm	2.6	2.4
λ^{-1}/nm	12	13
s/nm	1.31	1.38

[a]cited from ref 13. [b]cited from ref 14.

the present surfactant mixtures have similar characteristics to those of the corresponding single surfactant C_iE_j, except for the stiffness of the micelles of $C_{10}E_6 + C_{14}E_6$ with $w_t = 0.502$ and $C_{12}E_6$. The λ^{-1} value of the micelle of $C_{10}E_6 + C_{14}E_6$ ($w_t = 0.502$) is considerably larger than that of the $C_{12}E_6$ micelle.

CONCLUSION

In this work, we have studied the micelles of the binary surfactant mixtures of polyoxyethylene alkyl ethers $C_{10}E_6 + C_{14}E_6$ and $C_{14}E_8 + C_{14}E_6$ by static (SLS) and dynamic light scattering (DLS) experiments by employing the same technique as used in the previous studies.[13–17,19] The results of $Kc/\Delta R_0$ from SLS have been analyzed with the aid of the thermodynamic theory[20] for light scattering of micelle solutions formulated with wormlike spherocylinder model, thereby yielding the molar mass $M_w(c)$ as a function of c along with the cross-sectional diameter d of the micelle.

It has been found that the micellar length increases with increasing concentration c or with raising temperature T irrespective of the composition of the surfactant mixtures, as in the case of the micelles of the single surfactant C_iE_j with various i and j. The length of the micelles at fixed c and T steeply increases with increasing weight fraction w_t of $C_{14}E_6$ in both of the surfactant mixtures, implying that the micelles greatly grow in length when the surfactant component with longer alkyl group or with shorter oxyethylene group increases in the mixtures. The results are in line with the previous findings for the micelles of the single surfactant systems that the C_iE_j micelles grow in length to a greater extent for larger i and smaller j, since among surfactant molecules, attractive force due to the hydrophobic interactions becomes stronger for larger i and repulsive force due to the hydrophilic interactions becomes stronger for larger j.

The values of the cross-sectional diameter d of the cylindrical micelles and the spacing s between the adjacent surfactant molecules on the micellar surface do not significantly vary with composition of the surfactant mixture. On the contrary, the stiffness parameter λ^{-1} largely decreases with w_t, indicating that the stiffness of the micelle is controlled by the relative strength of the repulsive force due to the hydrophilic interactions between oxyethylen groups to the attractive one due to the hydrophobic interactions between alkyl groups among the surfactant molecules.

Acknowledgment. This research was supported in part by Nara Women's University Intramural Grant for Project Research.

REFERENCES

1. A. Bernheim-Groswasser, E. Wachtel, and Y. Talmon, *Langmuir*, **16**, 4131 (2000).
2. W. Brown, R. Johnson, P. Stilbs, and B. Lindman, *J. Phys. Chem.*, **87**, 4548 (1983).
3. T. Kato and T. Seimiya, *J. Phys. Chem.*, **90**, 1986 (1986).
4. W. Brown and R. Rymdén, *J. Phys. Chem.*, **91**, 3565 (1987).
5. W. Brown, Z. Pu, and R. Rymdén, *J. Phys. Chem.*, **92**, 6086 (1988).
6. T. Imae, *J. Phys. Chem.*, **92**, 5721 (1988).
7. W. Richtering, W. Burchard, and H. Finkelmann, *J. Phys. Chem.*, **92**, 6032 (1988).
8. T. Kato, S. Anzai, and T. Seimiya, *J. Phys. Chem.*, **94**, 7255 (1990).
9. H. Strunk, P. Lang, and G. H. Findenegg, *J. Phys. Chem.*, **98**, 11557 (1994).
10. P. Schurtenberger, C. Cavaco, F. Tiberg, and O. Regev, *Langmuir*, **12**, 2894 (1996).
11. G. Jerke, J. S. Pedersen, S. U. Egelhaaf, and P. Schurtenberger, *Langmuir*, **14**, 6013 (1998).
12. O. Glatter, G. Fritz, H. Lindner, J. Brunner-Papela, R. Mittelbach, R. Strey, and S. U. Egelhaaf, *Langmuir*, **16**, 8692 (2000).
13. S. Yoshimura, S. Shirai, and Y. Einaga, *J. Phys. Chem. B*, **108**, 15477 (2004).
14. N. Hamada and Y. Einaga, *J. Phys. Chem. B*, **109**, 6990 (2005).
15. K. Imanishi and Y. Einaga, *J. Phys. Chem. B*, **109**, 7574 (2005).
16. Y. Einaga, A. Kusumoto, and A. Noda, *Polym. J.*, **37**, 368 (2005).
17. Y. Shirai and Y. Einaga, *Polym. J.*, **37**, 913 (2005).
18. S. Shirai, S. Yoshimura, and Y. Einaga, *Polym. J.*, **38**, 37 (2006).
19. Y. Einaga, Y. Inaba, and M. Syakado, *Polym. J.*, **38**, 64 (2006).
20. T. Sato, *Langmuir*, **20**, 1095 (2004).
21. R. Koyama and T. Sato, *Macromolecules*, **35**, 2235 (2002).
22. H. Benoit and P. Doty, *J. Phys. Chem.*, **57**, 958 (1953).
23. T. Norisuye, M. Motowoka, and H. Fujita, *Macromolecules*, **12**, 320 (1979).
24. H. Yamakawa and M. Fujii, *Macromolecules*, **6**, 407 (1973).
25. H. Yamakawa and T. Yoshizaki, *Macromolecules*, **12**, 32

(1979).
26. T. Yoshizaki, T. Nitta, and H. Yamakawa, *Macromolecules*, **21**, 165 (1988).
27. B. Berne and R. Pecora, "Dynamic Light Scattering," J. Wiley, New York, 1976.
28. P. Štěpánek, W. Brown, and S. Hvidt, *Macromolecules*, **29**, 8888 (1996).
29. D. Blankschtein, M. Thurston, and G. B. Benedek, *J. Chem. Phys.*, **85**, 7268 (1986).
30. M. E. Cates and S. J. Candou, *J. Phys.: Condens. Matter*, **2**, 6869 (1990).
31. N. Zoeller, L. Lue, and D. Blankschtein, *Langmuir*, **13**, 5258 (1997).
32. K. Imanishi and Y. Einaga, to be published.
33. Y. Nakamura and T. Norisuye, *Polym. J.*, **33**, 874 (2001).
34. T. Sato, private communication.